JOURNAL OF VIROLOGY, June 1993, p. 3507–3514
0022-538X/93/063507-08$02.00/0

Vol. 67, No. 6

# The Adenovirus L3 23-Kilodalton Proteinase Cleaves the Amino-Terminal Head Domain from Cytokeratin 18 and Disrupts the Cytokeratin Network of HeLa Cells

PAUL H. CHEN,† DAVID A. ORNELLES, AND THOMAS SHENK*

*Department of Molecular Biology, Howard Hughes Medical Institute, Princeton University, Princeton, New Jersey 08544-1014*

Received 6 January 1993/Accepted 25 February 1993

**Immunofluorescence studies revealed that adenovirus induces a reorganization of the cytokeratin system in lytically infected HeLa cells. At 24 h postinfection, the cytokeratin network began to disassemble into prominent spheroid globules. By 36 h postinfection, host cell lysis occurred, accompanied by the formation of perinuclear cytokeratin clumps and additional spheroid globules. Immunoblots detected 41- and 44-kDa fragments of cytokeratin 18 and reduced levels of cytokeratin 7 at 24 and 36 h postinfection. Cytokeratin proteins isolated from HeLa cells at 36 h postinfection were deficient in filament polymerization. The 41-kDa proteolytic cytokeratin 18-specific fragment was purified, and its amino-terminal sequence was determined to be GGIQNEKETM. These residues correspond to amino acids 74 through 83 of cytokeratin 18, identifying a cleavage site at the junction of the globular head domain and the α-helical rod domain. Moreover, this truncation event occurs at a consensus cleavage site for the adenovirus L3 23-kDa proteinase. The temperature-sensitive mutant H2-*ts*1, which contains a mutation in the proteinase, neither induced cleavage of cytokeratin 18 nor precipitated the formation of spheroid globules during lytic infection at the nonpermissive temperature. The active proteinase is therefore required for cleavage of cytokeratin 18 and morphological rearrangement of the cytokeratins. We suggest that disruptions in the cytokeratin system weaken the mechanical integrity of the cell, thus promoting host cell lysis and release of progeny virions.**

Actin filaments, microtubules, and intermediate filaments are components of the cytoskeleton. The intermediate filaments include the cytokeratins which form a highly stable and unusually insoluble protein fiber network in the cytoplasm of epithelial cells, imparting mechanical integrity to the cell (9, 26). Different cytokeratin polypeptides all contain a conserved central region of about 310 amino acid residues that forms an extended α helix with three short non-α-helical interruptions. Long stretches of this conserved central region have repeated copies of a heptad repeat motif that forms a coiled coil (14). In contrast to the conserved central domain, the amino-terminal and carboxyl-terminal domains of intermediate filaments are non-α helical and vary greatly in size and sequence across different cytokeratin proteins (8). These variations in the head and tail domains allow one to classify cytokeratin proteins into two subfamilies, namely, the acidic or type I cytokeratins and the basic-to-neutral or type II cytokeratins. Type I cytokeratins exhibit immunological similarity and homology at the DNA level, and they tend to migrate as small, acidic polypeptides on a two-dimensional polyacrylamide gel. Type II cytokeratins likewise show immunological similarity and homology at the DNA level, but they migrate as larger, neutral-to-basic proteins (14).

The mechanism for filament formation has been elucidated in molecular detail. In the first step, an acidic cytokeratin aligns in parallel with a basic cytokeratin to yield a coiled-coil dimer. Next, a tetramer is formed by antiparallel, staggered side-by-side aggregation of two dimers. Tetramers polymerize end to end to form a protofilament, and eight protofilaments then combine to produce the final 10-nm filament (25). Cytokeratins with amino-terminal deletions are capable of coiled-coil and higher-ordered lateral interactions but are deficient in filament elongation (8).

In the adenovirus field, studies of virus-cytoskeleton interactions have focused on vimentin, another class of intermediate filament. The extended vimentin system has been shown to collapse into the perinuclear region in adenovirus-infected monkey (22), hamster (5), and human (10, 31) cells. Belin and Boulanger (5) have shown that cleavage is mediated by a cellular, $Ca^{2+}$-dependent enzyme. Vimentin cleavage products can be detected 5 min after addition of virus to a culture; as expected for a process that begins so rapidly, cleavage does not require viral gene expression since it is induced by empty viral particles (5). In a similar vein, White and Cipriani (27, 28) have shown that the vimentin system collapses into a juxtanuclear location when the adenovirus E1B 21-kDa oncoprotein is expressed in transfected cells. It is not clear whether cleavage occurs in this case.

This study further investigates the interaction of adenoviruses with the intermediate filament system of HeLa cells during lytic infection. Late during the infectious process, cytokeratin filaments are disassembled to form spheroid globules and cytoplasmic clumps. This alteration is due at least in part to the activity of the adenovirus L3 23-kDa proteinase which cleaves the cytokeratin 18 (K18) molecule, removing its amino-terminal head region and blocking its ability to assemble into fibers.

(This work forms a portion of the senior thesis of P. H. Chen at Princeton University.)

## MATERIALS AND METHODS

**Cells and viruses.** HeLa cell strain CCL2.2 was obtained from the American Type Culture Collection (Rockville, Md.)

* Corresponding author.
† Present address: Harvard Medical School, Boston, MA 02115-5750.

and maintained in monolayers with Dulbecco modified Eagle's minimal essential medium supplemented with 10% calf serum (GIBCO Laboratories, Grand Island, N.Y.). The phenotypically wild-type adenovirus type 5, H5*dl*309, was used in all experiments (16) except those employing H2-*ts*1 (29) and its wild-type adenovirus type 2 (Ad2) parent. To produce stocks of phenotypically wild-type viruses, infections were allowed to proceed at 37°C for 48 h, and stocks of H2*ts*-1 were made after maintaining infected cells at 32°C for 84 h. After harvesting, cells were disrupted by sonication, and virions were purified by sequential centrifugation in discontinuous and equilibrium $CsCl_2$ gradients. Virion concentrations were determined by measuring $A_{260}$.

**Immunofluorescence.** For time course immunofluorescence studies, HeLa cells were seeded at a 1:10 dilution onto polylysine-treated, 10-well glass microscope slides 24 h before infection. For immunofluorescence experiments using temperature-sensitive mutants, cells were seeded at a 1:10 dilution onto 10-cm-diameter tissue culture dishes. Cultures were infected at a multiplicity of 2,000 virions per cell in phosphate-buffered saline (PBS; 137 mM NaCl, 3 mM KCl, 16 mM $Na_2HPO_4$, 2 mM $KH_2PO_4$) supplemented with 2% calf serum, 1 mM $CaCl_2$, and 1.5 mM $MgCl_2$.

At the appropriate time postinfection, cells were washed three times with PBS containing 1.5 mM $MgCl_2$ (PBS + Mg) and fixed in 4% formaldehyde in PBS + Mg (prepared immediately before use) for 10 min at room temperature. Specimens were again washed three times with PBS + Mg and permeabilized with 0.2% Triton X-100 in PBS + Mg for 5 min at room temperature. Next, the cells were washed five times with Tris-buffered saline (TBS; 20 mM Tris-Cl [pH 7.6], 137 mM NaCl, 3 mM KCl, 1.5 mM $MgCl_2$) containing 5 mg of bovine serum albumin per ml, 1 mg of glycine per ml, and 0.05% sodium azide (TBS-BG) with 0.05% Tween 20. Samples were incubated in buffer containing the primary antibody for 3 h at room temperature within a humidified chamber. After primary antibody binding took place, the samples were washed five times in TBS-BG with 0.05% Tween 20 and incubated with secondary antibodies for 30 min. Double-label-grade fluorescein-conjugated goat anti-mouse immunoglobulin G (IgG; Jackson ImmunoResearch, West Grove, Pa.) and double-label-grade Texas red-conjugated goat anti-rat IgG (Jackson ImmunoResearch) were used at 15 μg/ml in TBS-BG with 0.05% Tween 20 and 10% goat serum. After being washed five times in TBS-BG with 0.05% Tween 20 and 10% goat serum, the samples were mounted in PBS-glycerol containing 10% polyvinyl alcohol and 1 mg of *p*-phenylenediamine per ml. Samples were examined and photographed with a Zeiss Photomicroscope III under epifluorescence illumination. Exposures were standardized for each experiment and were typically between 10 and 45 s with Kodak T-Max 400 film (Eastman Kodak, Rochester, N.Y.) developed to an effective exposure index of 800 by using T-Max liquid developer.

The following primary antibodies were used for immunofluorescence. Rat IgG monoclonal antibody 9C10 (Oncogene Sciences, Manhasset, N.Y.), which recognizes the E1B 55-kDa protein (30), was used at a 1:10 dilution. Mouse IgG monoclonal antibody KS-B17.2 (Sigma, St. Louis, Mo.), which reacts exclusively with K18, was used at a 1:20 dilution. Mouse IgG monoclonal antibody M20 (Sigma), which binds specifically to K8, was used at a 1:20 dilution. All antibodies were diluted in TBS-BG with 0.05% Tween 20 and 10% goat serum.

**Western immunoblotting.** Protein samples from uninfected or adenovirus-infected cells were normalized for a standardized number of cells, denatured by sodium dodecyl sulfate (SDS) treatment, and separated by electrophoresis on a 10% polyacrylamide gel. Polypeptides were electrophoretically transferred to nitrocellulose paper in transfer buffer (20 mM Tris, 150 mM glycine, 20% methanol) at 0.9 A for 3 h at 4°C. Protein bands were stained with 0.1% amido black and destained with 10% acetic acid–50% methanol. Samples destined for immunoblots were blocked overnight with 5% nonfat dry milk in PBS. Blots were incubated with the primary antibody for 3 h at room temperature. Antigen-antibody complexes were then incubated with bacterial alkaline phosphatase-conjugated goat anti-mouse secondary antibody (Sigma) and visualized by adding AP buffer (0.1 M Tris-Cl [pH 9.5], 0.1 M NaCl, 10 mM $MgCl_2$) with 0.3 mg of 5-bromo-4-chloro-3-indolyl phosphate per ml and 0.15 mg of nitroblue tetrazolium per ml. Development was stopped by washing the blot in 10 mM Tris (pH 7.6)–1 mM EDTA.

The following primary antibodies were used for blotting experiments. Mouse IgG monoclonal antibody 8.13 (Sigma), which recognizes cytokeratins K1, K5, K6, K7, K8, K10, K11, and K18 (13), was used at a 1:200 dilution. Mouse IgG antibody CY-90 (Sigma), which recognizes K18 exclusively, was used at a 1:1,000 dilution. Mouse IgG antibody RPN.1102 (Amersham, Amersham, England), which reacts exclusively with vimentin, was used at a 1:50 dilution. Mouse IgG antibody C4 (Boehringer, Mannheim, Germany), which binds specifically to actin, was used at a 1:600 dilution. Antibodies were diluted in TBS-BG with 0.05% Tween 20 and 10% goat serum. Mouse IgG antibody B6-8, which recognizes the adenovirus E2A 72-kDa protein (18), was kindly provided by A. J. Levine (Princeton University) and used as an undiluted tissue culture supernatant.

**Cellular fractionation scheme.** Samples were biochemically fractionated by sequential extraction. Cells were washed in PBS + Mg and extracted with CSK buffer [100 mM KCl, 300 mM sucrose, 3 mM $MgCl_2$, 1 mM ethylene glycol-bis(β-aminoethyl ether)-*N*,*N*,*N*′,*N*′-tetraacetic acid (EGTA), 10 mM piperazine-*N*,*N*′-bis(2-ethanesulfonic acid) (PIPES) buffer (pH 6.8), 0.5% Triton X-100, 1.2 mM phenylmethylsulfonyl fluoride (PMSF)] for 5 min on ice, which removes most of the phospholipids and about 65% of the total cell protein in the soluble fraction (12). Cells were then treated with extraction buffer (250 mM ammonium sulfate, 300 mM sucrose, 3 mM $MgCl_2$, 1 mM EGTA, 10 mM PIPES buffer [pH 6.8], 0.5% Triton X-100, 1.2 mM PMSF) for 5 min on ice to remove salt-labile proteins, noncore histones, polyribosomes, and most of the extractable actin in the cytoskeletal fraction. Next, samples were incubated in digestion buffer (50 mM NaCl, 300 mM sucrose, 3 mM $MgCl_2$, 1 mM EGTA, 10 mM PIPES buffer [pH 6.8], 0.5% Triton X-100, 1.2 mM PMSF) with 200 μg of DNase I per ml and 200 μg of RNase A per ml for 30 min at room temperature. Cells were treated again with extraction buffer for 5 min at room temperature, releasing the nucleic acids, chromatin-associated proteins, and heterogeneous nuclear ribonucleoprotein-associated proteins in the chromatin fraction. The remaining material was greatly enriched for the nuclear matrix-intermediate filament scaffold of the cell. The cytoskeletal, chromatin, and nuclear matrix-intermediate filament fractions represent 23, 7, and 5% of the total cell protein, respectively (12).

**In vitro disassembly-assembly of intermediate filaments.** The nuclear matrix-intermediate filament fraction was dissolved in disassembly buffer (8 M urea, 20 mM PIPES buffer [pH 6.8], 1 mM EGTA, 1 mM PMSF, 0.1 mM $MgCl_2$, 1% β-mercaptoethanol) by sonication. Samples were then cleared by centrifugation at 250,000 × *g* for 1 h at 15°C. To

allow reassembly of filaments, the cleared supernatant was dialyzed for 12 h at 25°C against a 1,000× volume of assembly buffer (150 mM KCl, 25 mM imidazole-HCl [pH 7.1], 5 mM $MgSO_4$, 2 mM dithiothreitol, 125 μM EGTA, 0.2 mM PMSF). Filaments were harvested by centrifugation at 150,000 × *g* for 45 min at 25°C. Both the pellet and the supernatant were saved for analysis.

**Amino-terminal protein sequencing.** Protein samples were concentrated by acetone precipitation, denatured by SDS treatment, and separated by electrophoresis in a 10% polyacrylamide gel with 0.1 mM thioglycolate added to the running buffer to scavenge reactive contaminants. After separation, polypeptides were transferred onto polyvinylidene difluoride membranes (Bio-Rad, Richmond, Calif.) in CAPS buffer (10 mM 3-cyclohexylamino-1-propanesulfonic acid [pH 11], 10% methanol) by electrophoresis at 50 V for 45 min at room temperature. Protein bands were stained for 1 h with 0.025% Coomassie blue in 40% methanol and destained with 50% methanol. Bands of interest were excised and sequenced by Edman degradation on a model 473A automated protein sequenator (Applied Biosystems, Foster City, Calif.).

## RESULTS

**Adenovirus infection induces a reorganization of the cytokeratin system.** Indirect immunofluorescence was used to examine the morphological arrangement of the cytokeratin system in adenovirus-infected HeLa cells. The cytokeratins were probed with mouse monoclonal antibody KS-B17.2, which specifically recognizes K18, or mouse monoclonal antibody M20, which reacts exclusively with K8. Immunofluorescent images obtained by using KS-B17.2 were indistinguishable from images obtained by using M20. The progress of infection was monitored by double-label immunofluorescence with rat monoclonal antibody 9C10, which specifically recognizes the adenovirus E1B 55-kDa protein (30).

Mock-infected HeLa cells exhibited a normal filamentous cytokeratin network extending throughout the cytoplasm (Fig. 1A). At 12 h postinfection, the cytokeratins still appeared essentially normal (Fig. 1B), and the presence of the E1B 55-kDa polypeptide demonstrated that the cells were properly infected (data not shown). A striking change was evident at 24 h postinfection. The cytokeratin system began to disassemble into prominent spheroid globules spread throughout the cytoplasm of the cells (Fig. 1C). Residual cytokeratin filaments were nonetheless still visible at this time, especially in the perinuclear region. By 36 h postinfection, cytokeratin disassembly was complete. The rounded cells (Fig. 1D) contained extensive spheroid globules throughout their cytoplasm, with no apparent cytokeratin filaments remaining. Other infected HeLa cells exhibited cytoplasmic cytokeratin clumps that stained intensely under immunofluorescence (Fig. 1E). Extensive cell lysis occurred by this time, leaving assorted cytokeratin debris on the surface of the microscope slide (Fig. 1F). These morphological perturbations in the cytokeratin system occurred with variable frequency, ranging in repeated experiments from 20 to 60% of the total population of infected cells at 36 h postinfection.

**Proteolysis of K18 and reduced levels of K7 at 36 h postinfection with adenovirus.** Western blots were performed to elucidate the biochemical basis for the observed morphological rearrangement. Cytokeratin-specific monoclonal antibodies were used to probe whole-cell protein samples from mock-infected cells, as well as cells at 12 h, 24 h, and 36 h postinfection. Since cytokeratins K7, K8, and K18 comprise the major keratin species in HeLa cells (24), samples were first examined with the broad-range monoclonal antibody 8.13, which recognizes K1, K5, K6, K7, K8, K10, K11, and K18 (13). Western blotting with antibody 8.13 (Fig. 2A) revealed that substantial amounts of K7, K8, and K18 were present in mock-infected cells, and the normal expression pattern persisted through 12 h postinfection. At 24 h postinfection, the levels of K8 and K18 were still comparable to those in the mock-infected samples, but the signal for full-length K7 dropped perceptibly and novel 41- and 44-kDa cytokeratin-specific fragments appeared. By 36 h postinfection, K7 levels were reduced even further, the 41-kDa fragment became more prominent, and the 44-kDa fragment was barely detectable.

Monoclonal antibodies specific to individual cytokeratins were used to ascertain the identity of the 41- and 44-kDa cytokeratin-specific fragments. Both fragments were recognized by antibody CY-90 (Fig. 2B). Since CY-90 binds specifically to K18 in mock-infected and 12-h postinfection samples, the observed immunological recognition strongly suggests that the 41- and 44-kDa fragments are specific proteolytic breakdown products of K18. Cleavage of K18 must be rather inefficient, because appreciable amounts of full-length K18 remain at 24 and 36 h postinfection (Fig. 2B). As a control, the course of viral infection was monitored with monoclonal antibody B6-8 (18), which binds exclusively to the adenovirus E2A 72-kDa protein. No E2A 72-kDa protein was present in mock-infected cells, while increasing amounts were seen at 12, 24, and 36 h postinfection (Fig. 2C).

**Cytokeratin proteins from cells at 36 h postinfection are deficient in filament polymerization.** Since we had already established that adenovirus infection induces molecular and morphological perturbations to the cytokeratin system, we proceeded to investigate the effect of adenovirus infection on the polymerization of cytokeratin proteins. Mock-infected HeLa cells and HeLa cells at 36 h postinfection were sequentially extracted to the nuclear matrix-intermediate filament scaffolding, which greatly enriches for cytokeratin polypeptides (12). After these samples were dissolved in 8 M urea, the proteins were allowed to repolymerize by dialysis against assembly buffer. Reassembled filaments were pelleted by centrifugation, leaving unpolymerized proteins in the supernatant.

The pellet and supernatant fractions of both uninfected and infected cells were analyzed by Western blots. Immunoblots probed with antibody 8.13 revealed that high levels of K7, K8, and K18 were present in the pellet fraction but not in the supernatant fraction of uninfected cells (Fig. 3A), indicating that cytokeratin proteins from mock-infected HeLa cells are fully competent for in vitro filament polymerization. In contrast, the samples prepared from cells at 36 h postinfection contained significant amounts of K8, K18, and proteolyzed K18 in both the pellet and supernatant fractions (Fig. 3A). Therefore, the cytokeratin proteins of HeLa cells at 36 h postinfection appear to be functionally deficient in filament formation.

The polymerization competence of vimentin, another intermediate filament protein present in HeLa cells, was assessed by using monoclonal antibody RPN.1102 (Fig. 3B). For mock-infected cells, large quantities of vimentin were observed in pellet fraction, while little signal was detected in the supernatant fraction. Samples from 36 h postinfection also exhibited a high concentration of vimentin protein in the pellet, with only trace amounts of vimentin present in the supernatant. Since vimentin repolymerizes effectively in both mock-infected and infected samples, we conclude that the inhibition of cytokeratin filament polymerization in infected cells is a specific effect that does not extend to all intermediate filaments present in the host cell.

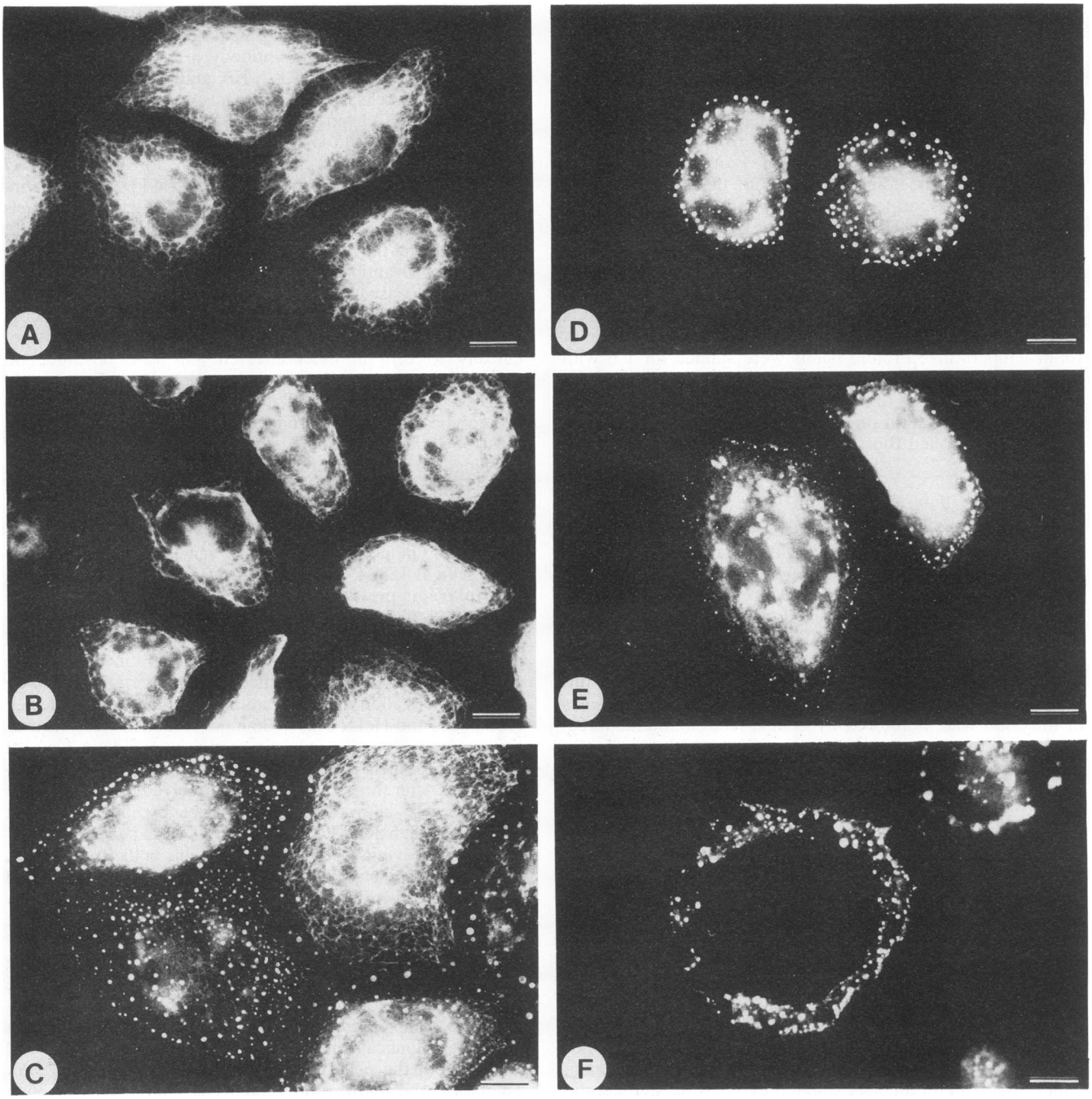


FIG. 1. Time course immunofluorescence analysis of uninfected and adenovirus-infected HeLa cells with use of a cytokeratin-specific antibody. Cells were grown on polylysine-treated glass slides and then mock infected or infected with 2,000 virions per cell. At various times after infection, cells were fixed, permeabilized, and processed for indirect immunofluorescence using mouse monoclonal antibody KS-B17.2, which specifically recognizes the K18 polypeptide. (A) Mock-infected cells; (B) cells at 12 h postinfection; (C) cells at 24 h postinfection; (D to F) cells at 36 h after infection. Bars, 10 μm.

**Cleavage occurs at an adenovirus L3 23-kDa proteinase recognition site, removing the head domain from K18.** The protocol used to assess competence for filament polymerization also served as a purification scheme to isolate cytokeratin proteins from infected HeLa cells. Sequential extraction to the nuclear matrix-intermediate filament scaffold removes 95% of all cellular proteins yet preserves 99% of keratin proteins present in the cell (12). Unfortunately, residual amounts of actin often remain in the nuclear matrix-intermediate filament fraction (7). Since the molecular size of actin is 42 kDa (2), it would migrate very near, and likely contaminate, the 41- and 44-kDa proteolytic fragments of K18 separated by polyacrylamide gel electrophoresis. One cycle of filament disassembly-assembly afforded an additional degree of purification, since actin segregated completely into the pellet fraction for both mock-infected and infected samples

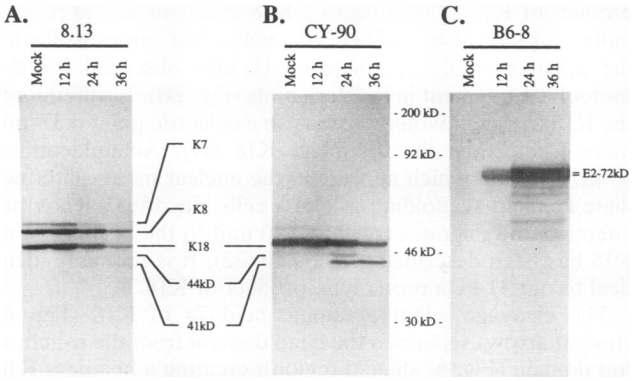


FIG. 2. Time course immunoblot analysis of uninfected and adenovirus-infected HeLa cells. Whole-cell protein samples derived from mock-infected cells as well as cells at 12 or 36 h postinfection were probed with several monoclonal antibodies. Cytokeratin proteins were visualized with either antibody 8.13, which recognizes K7, K8, K18, and the 41-kDa cytokeratin-specific fragment (A), or the more specific antibody CY-90, which reacts exclusively with K18 and the 41-kDa cytokeratin-specific fragment (B). (C) The course of viral infection was monitored by using antibody B6-8, which interacts with the adenovirus E2A 72-kDa polypeptide. Bands representing cytokeratin-specific polypeptides and the adenovirus E2A 72-kDa protein, as well as the positions of markers, are labeled.

(Fig. 3C). Indeed, amido black staining of total protein revealed that few proteins were left in the supernatant fraction of mock-infected and infected samples (Fig. 3D). The supernatant fraction of the 36-h postinfection sample therefore contained significant amounts of K8, K18, and 41-kDa proteolytic fragment (Fig. 3A) with little contaminating vimentin (Fig. 3B), actin (Fig. 3C), or other proteins (Fig. 3D).

The purified 41-kDa cytokeratin fragment was subjected to Edman degradation using a gas-phase protein sequenator. Its first 10 amino-terminal residues were GGIQNEKETM, precisely matching amino acids 74 through 83 of cytokeratin K18, located at the junction of its globular head and α-helical rod domains. Moreover, this sequence corresponded to an adenovirus L3 23-kDa proteinase consensus cleavage site (3).

We were unable to obtain unambiguous sequencing information on the minor 44-kDa proteolytic fragment, probably because of contamination from the more abundant 41-kDa fragment in the 36-h sample preparations.

**H2-*ts*1 neither induces proteolysis of K18 nor precipitates the formation of spheroid globules at the nonpermissive temperature.** The adenovirus mutant H2-*ts*1 contains a proline-to-leucine substitution at amino acid 63 of the L3 23-kDa polypeptide, which confers temperature sensitivity upon the viral proteinase of this mutant (29). To test whether the viral proteinase did indeed cleave cytokeratin K18, HeLa cells were infected with either H2-*ts*1 or its wild-type parent and then maintained at either the restrictive (39.5°C) or permissive (32°C) temperature. Cells were collected and processed for Western blot analysis after 20 h for the 39.5°C samples or 84 h for the 32°C samples.

Immunoblotting with monoclonal antibody CY-90 (Fig. 4) revealed that proteolysis of K18 occurred in H2-*ts*1-infected cells grown at the permissive temperature but not in H2-*ts*1-infected cells grown at the nonpermissive temperature. In contrast, cells infected with the wild-type Ad2 exhibited proteolysis of K18 regardless of whether the cells were maintained at 32 or 39.5°C. These data demonstrate that the active adenovirus proteinase is necessary for efficient cleavage of the K18 peptide.

The essential role of the adenovirus proteinase was underscored in a parallel set of immunofluorescence experiments. H2-*ts*1-infected cells contained spherical globules when maintained at the permissive temperature (Fig. 5A), while at the restrictive temperature, H2-*ts*1-infected cells exhibited no reorganization of their cytokeratin systems (Fig. 5B). On the other hand, cells infected with the parental Ad2 developed spherical globules when propagated at both 32°C (Fig. 5C) and 39.5°C (Fig. 5D). Thus, the active adenovirus proteinase is required for morphological rearrangement of the cytokeratin network.

## DISCUSSION

The amino-terminal residues of the 41-kDa cytokeratin fragment matched amino acids 74 through 83 of cytokeratin K18 (Fig. 6, bold italics), confirming that it is a proteolytic

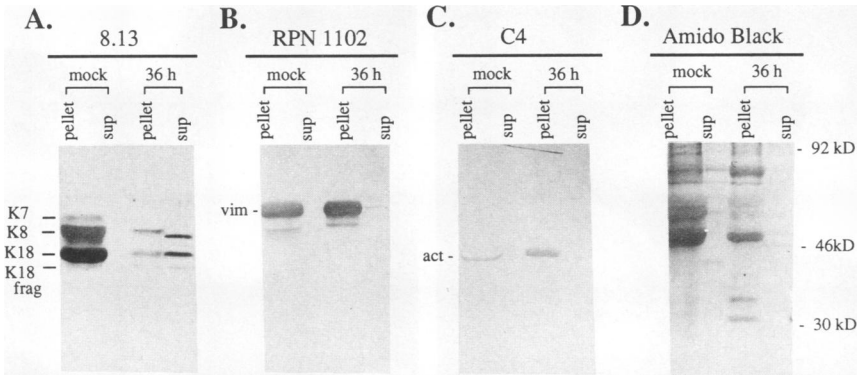


FIG. 3. In vitro disassembly-assembly assay. Intermediate filaments were extracted from mock-infected HeLa cells or cells at 36 h postinfection and subjected to one cycle of in vitro disassembly-assembly. Reassembled filaments were pelleted by ultracentrifugation, leaving soluble proteins in the supernatant (sup). Both soluble and pellet fractions were subjected to polyacrylamide gel electrophoresis, and proteins were electrophoretically transferred to nitrocellulose. Three identical blots were probed with monoclonal antibody 8.13, which recognizes K7, K8, K18, and the 41-kDa cytokeratin-specific fragment (A), monoclonal antibody RPN.1102, which recognizes vimentin, a related intermediate filament protein (B), or monoclonal antibody C4, which recognizes actin (C). (D) Total protein was monitored by staining a fourth blot with amido black. Cytokeratin, vimentin (vim), and actin (act) bands, as well as the positions of markers, are labeled.

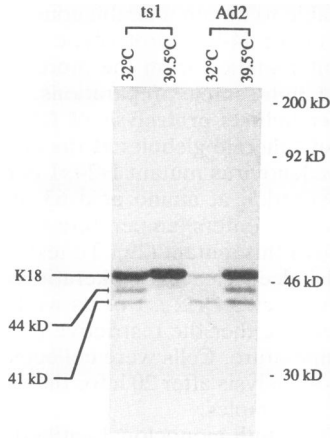


FIG. 4. Immunoblot analysis of K18 expression in HeLa cells infected with H2-*ts*1 or Ad2. HeLa cells were infected with 2,000 virions of H2-*ts*1 or the wild-type Ad2 parent per cell. Infection was allowed to proceed at either 32°C for 84 h or 39.5°C for 20 h. Whole-cell protein samples were electrophoretically separated, blotted, and probed with antibody CY-90. Bands representing K18 and K18-specific fragments, as well as the positions of markers, are labeled.

product of K18. The truncated K18 fragment would have a molecular size of 40.8 kDa (11), a value that agrees well with the apparent molecular size of 41 kDa observed for the proteolytic fragment in Western blots (Fig. 2B). Furthermore, the K18 fragment would possess an isoelectric point 0.37 unit more acidic than that of intact K18 (11). An unidentified 40-kDa protein which appears in the nuclear matrix-intermediate filament scaffolding of HeLa cells late after adenovirus infection and migrates roughly 0.40 unit to the acidic side of K18 has been described previously (32). It is probably identical to our 41-kDa proteolytic product of K18.

The cleavage event at amino acid 74 of K18 (Fig. 6, straight arrow) separates the head domain from the α-helical rod domain (Fig. 6, shaded region), creating a headless K18 protein. Transfection of cDNAs coding for full-length K8 and headless K18 into mouse 3T3-L1 cells, which normally express no cytokeratins, induces the formation of cytokeratin clumps and spheroid globules (4). The cytokeratin patterns in the transfected cells thus bear a marked resemblance to the spheroid globules (Fig. 1D) and cytoplasmic clumps (Fig. 1E) that we observe in adenovirus-infected HeLa cells. The start site of the transfected headless K18 at amino acid 83 (Fig. 6, bent arrow) lies only nine amino acids away from the site of adenovirus-induced K18 cleavage at amino acid 74 (Fig. 6, straight arrow). The situations are not entirely anal-

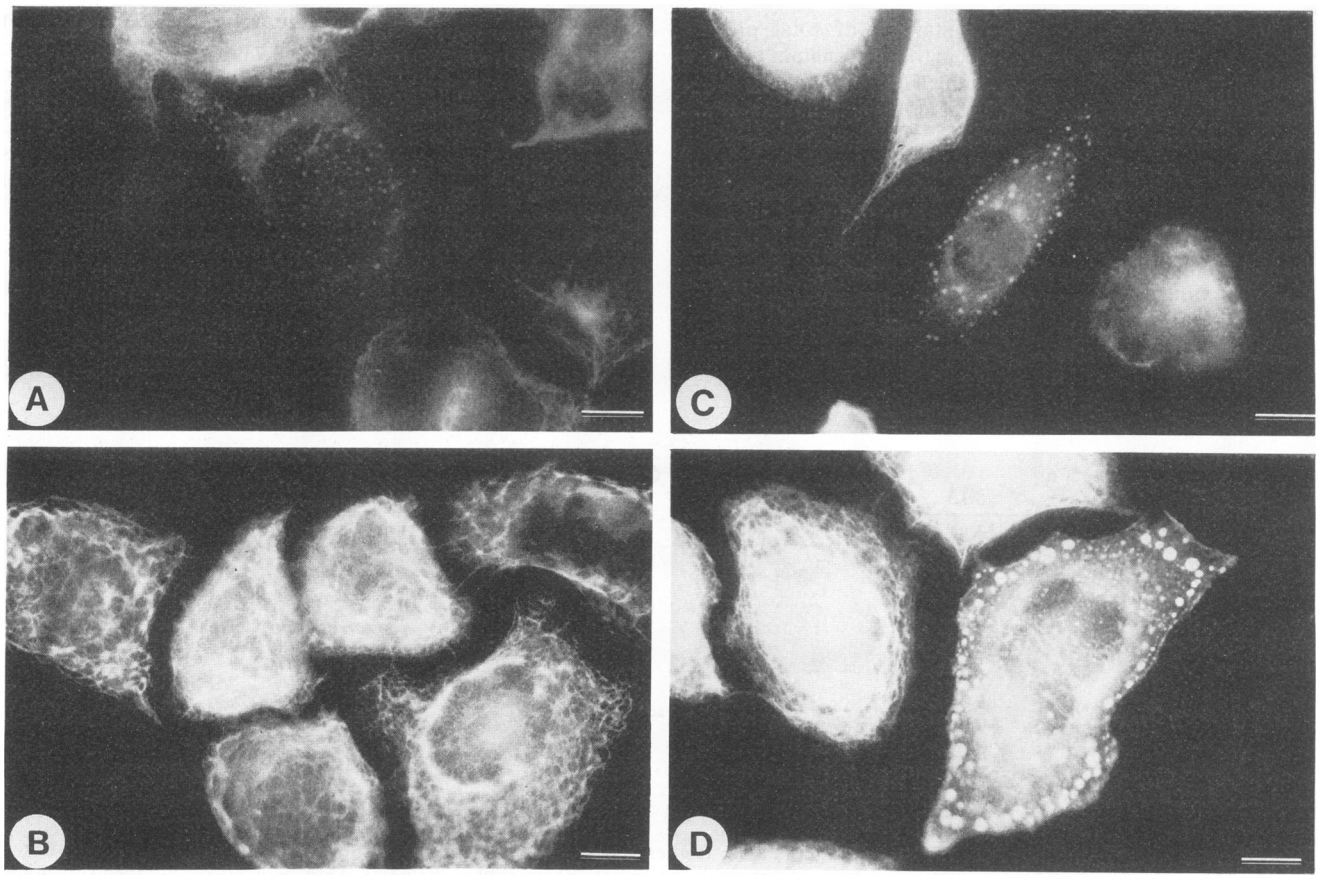


FIG. 5. Immunofluorescence analysis of HeLa cells infected with H2-*ts*1 or Ad2, using cytokeratin-specific antibodies. HeLa cells were infected with 2,000 virions of H2-*ts*1 or its wild-type Ad2 parent per cell. Infection was allowed to proceed at either 32°C for 84 h or 39.5°C for 20 h, and then cells were fixed, permeabilized, and processed for immunofluorescence. The cytokeratin system was probed with mouse monoclonal antibody M20, which specifically recognizes the K8 protein. (A) H2-*ts*1-infected cells at 32°C; (B) H2-*ts*1-infected cells at 39.5°C; (C) Ad2-infected cells at 32°C; (D) Ad2-infected cells at 39.5°C. Bars, 10 μm.

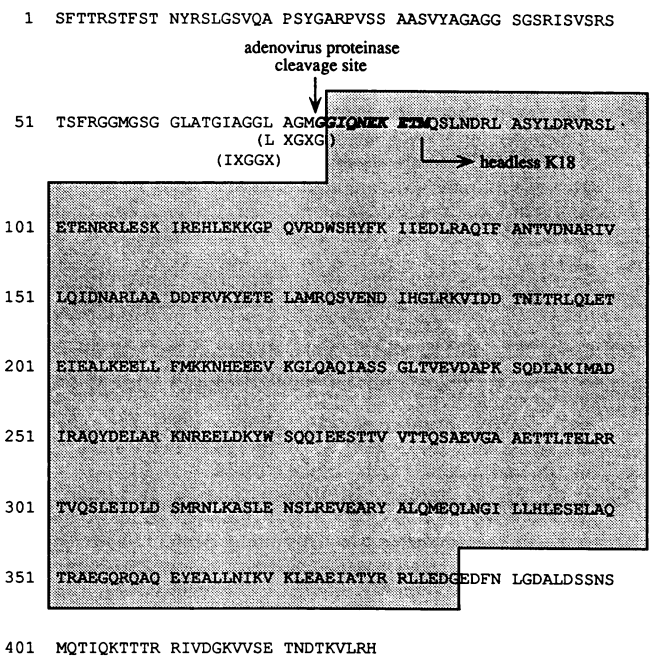


FIG. 6. Amino acid sequence of the K18 protein. The stippled region denotes the central α-helical rod domain, which is preceded by the globular head domain and followed by the globular tail domain. Bold italic type highlights the 10 amino acids of K18 which match the amino-terminal sequencing data. Appropriate versions of the adenovirus proteinase consensus sequence are aligned in parentheses below their corresponding amino acids in the K18 peptide. The straight arrow identifies the adenovirus proteinase cleavage site which generated the 41-kDa keratin fragment. The bent arrow denotes the start site of the headless K18 constructed by Bader et al. (4) for transfection into 3T3-L1 cells.

ogous because the transfection experiment constructs a de novo cytokeratin system in 3T3-L1 fibroblasts, whereas the adenovirus-induced cleavage occurs against a background of wild-type cytokeratins. However, transfection of the kidney epithelial cell line PtK2 with cDNAs coding for an amino-terminally deleted K14 polypeptide disrupts the endogenous K7, K8, K18, and K19 filament system into filamentous fragments and spheroid bodies, demonstrating that the phenotype for truncated cytokeratins can be dominant over the phenotype for full-length, wild-type cytokeratins (1).

It is well established that cytokeratins with amino-terminal deletions are capable of coiled-coil and higher-ordered lateral interactions but are deficient in filament elongation. In fact, cytokeratins with amino-terminal deletions significantly inhibit the elongation of wild-type cytokeratins, even when the mutant cytokeratin comprises only 1% of the total type I cytokeratin in the assembly mix (8). Therefore, headless K18 protein is likely to be a crucial factor for the inhibition of filament polymerization at 36 h postinfection. The reduced concentration of full-length K7 might also impair filament polymerization, although the chemical basis for such an effect remains unclear at this point.

Examination of the amino acid sequence in the vicinity of the cleavage site on K18 reveals two matches to the adenovirus proteinase consensus sequence, which has the generalized form (I/L/M)XGG ↓ X and (I/L/M)XGX ↓ G (3). In particular, K18 conforms to the proteinase recognition sequence IXGG ↓ X at amino acids 66 through 70 (Fig. 6, parentheses), and it also contains the proteinase recognition sequence LXGX ↓ G at amino acids 70 through 74 (Fig. 6, parentheses). Cleavage of K18 by the adenovirus proteinase at the latter consensus sequence site (Fig. 6, straight arrow) would be expected to yield a headless cytokeratin protein with an amino-terminal sequence of GGIQNEKETM (Fig. 6, bold italics), a predication consistent with our sequencing data. We therefore have strong evidence that the adenovirus proteinase cleaves K18 at the consensus sequence LXGX ↓ G. It is still unknown whether cleavage also occurs at the upstream consensus sequence IXGG ↓ X.

In addition to its effect on K18, the adenovirus proteinase might be responsible for the disappearance of full-length cytokeratin K7. Inspection of the K7 amino acid sequence (11) yields two matches to the adenovirus proteinase consensus sequence LXGX ↓ G, one in the head domain at amino acids 38 through 42 and one in the tail domain at amino acids 402 through 406. Given our evidence that the adenovirus proteinase cleaves at LXGX ↓ G in the K18 peptide, it is tempting to speculate that cleavage at one or both of the LXGX ↓ G sites present in the K7 peptide leads to the observed dramatic loss of full-length K7 protein (Fig. 2A).

Proteinase enzyme activity does not reach a maximum until 20 h postinfection (6), a time that correlates well with the appearance of spheroid globules, truncated cytokeratins, and deficient polymerization at 24 and 36 h postinfection. The experiments with H2-*ts*1 further implicate the adenovirus proteinase as a causative factor in the reorganization of the cytokeratin system. Lytic infection with H2-*ts*1 at the restrictive temperature neither precipitates the cleavage of K18 (Fig. 4) nor causes the formation of spheroid keratin globules (Fig. 5B), which demonstrates that the active adenovirus proteinase is necessary for efficient induction of perturbations to the cytokeratin system.

Our data identify a previously undiscovered role for the adenovirus proteinase. Expression of the proteinase late in the viral life cycle leads to truncation of cytokeratin K18 at the proteinase recognition sequence LXGX ↓ G, creating a 41-kDa headless K18. The proteinase probably also reduces the level of full-length cytokeratin K7 by cleaving at one or both of the LXGX ↓ G sites present in the head and tail domains. The truncation events severely disrupt the filament-forming capability of the keratin proteins in vitro and presumably also in vivo. The inability to form filamentous polymers then induces a morphological disassembly of the cytokeratin network into spheroid globules and cytoplasmic clumps.

A normal cytokeratin system helps to maintain the mechanical integrity of epithelial cells, while morphological perturbations to the cytokeratin network can lead to cytolysis (9, 26). Disassembly of the cytokeratin network during the late phase of adenovirus infection could make the host epithelial cell more susceptible to mechanical rupture and thus facilitate the release of progeny virion particles. Such a strategy would clearly enhance viral spread and may indeed influence pathogenesis. Histological samples derived from infant respiratory tracts after fatal adenovirus infection exhibit extensive destruction of bronchial epithelium and bronchial glands (23), an interesting observation in light of the fact that bronchial epithelium is known to contain both K7 and K18 proteins (17).

Recent reports indicate that human immunodeficiency virus type 1 (HIV-1) may pursue a similar strategy. The HIV-1 protease cleaves the intermediate filament proteins vimentin, desmin, and glial fibrillary acidic protein (19). Further studies focusing on vimentin indicate that a single site in the head domain acts as the primary cleavage site, and

three sites in the tail domain function as secondary cleavage sites (19). Filaments formed in vitro from the carboxyl-terminally truncated vimentin show a strong propensity to form large lateral aggregates, while vimentin lacking both head and tail domains fails to form filaments at all (21). Moreover, injection of the HIV-1 protease into cultured human fibroblasts results in a large increase in the percentage of cells exhibiting collapsed vimentin networks (20). The authors speculate that these changes could influence the release of virions from the plasma membrane during the budding process (21). Although the HIV-1 protease and the adenovirus proteinase recognize radically different sequences (15), the two viral enzymes seem to induce similar biochemical and morphological perturbations to the intermediate filament systems of their host cells. The collective data for HIV-1 and adenovirus thus elucidate a common theme in which diverse classes of viruses facilitate their propagation by proteolyzing the structural systems of their host cells.

## ACKNOWLEDGMENTS

Protein sequencing was performed by M. Flocco and B. Devlin at the Princeton Protein Sequencing Facility. Antibody B6-8 was provided by A. J. Levine. We are grateful for valuable discussions with E. Fuchs, S. J. Flint, and members of our laboratory.

This work was supported by grant CA 41086 from the National Cancer Institute. P. H. Chen received a summer stipend from the Howard Hughes Medical Institute. D. A. Ornelles is an associate of the Howard Hughes Medical Institute. T. Shenk is an American Cancer Society Professor and Investigator of the Howard Hughes Medical Institute.

## REFERENCES

1. **Albers, K., and E. Fuchs.** 1989. Expression of mutant keratin cDNAs in epithelial cells reveals possible mechanisms for initiation and assembly of intermediate filaments. J. Cell Biol. **108:**1477–1493.
2. **Alberts, B., D. Bray, J. Lewis, M. Raff, K. Roberts, and J. Watson.** 1989. The molecular biology of the cell. Garland Publishing, New York.
3. **Anderson, C.** 1990. The proteinase polypeptide of adenovirus serotype 2 virions. Virology **177:**259–272.
4. **Bader, B., T. Magin, S. Freudenmann, and W. Franke.** 1991. Intermediate filaments formed de novo from tail-less cytokeratins in the cytoplasm and in the nucleus. J. Cell Biol. **115:**1293–1307.
5. **Belin, M., and P. Boulanger.** 1987. Processing of vimentin occurs during the early stages of adenovirus infection. J. Virol. **61:**2559–2566.
6. **Bhatti, A., and J. Weber.** 1979. Protease of adenovirus type 2: partial characterization. Virology **96:**478–485.
7. **Capco, D., K. Wan, and S. Penman.** 1982. The nuclear matrix: three-dimensional architecture and protein composition. Cell **29:**847–858.
8. **Coulombe, P., Y. Chan, K. Albers, and E. Fuchs.** 1990. Deletions in epidermal keratins leading to alterations in filament organization in vivo and in intermediate filament assembly in vitro. J. Cell Biol. **111:**3049–3064.
9. **Coulombe, P., M. Hutton, R. Vassar, and E. Fuchs.** 1991. A function for keratins and a common thread among different types of epidermolysis bullosa simplex diseases. J. Cell Biol. **115:**1661–1674.
10. **Defer, C., M. Belin, M. Caillet-Boudin, and P. Boulanger.** 1990. Human adenovirus-host cell interactions: comparative study with members of subgroups B and C. J. Virol. **64:**3661–3673.
11. **Devereux, J., P. Haeberli, and O. Smithies.** 1984. A comprehensive set of sequence analysis programs for the VAX. Nucleic Acids Res. **12:**387–395.
12. **Fey, E., K. Wan, and S. Penman.** 1984. Epithelial cytoskeletal framework and nuclear matrix-intermediate filament scaffold: three dimensional organization and protein composition. J. Cell Biol. **98:**1973–1984.
13. **Gigi, O., B. Geiger, Z. Eshhar, R. Moll, E. Schmid, S. Winter, D. Schiller, and W. Franke.** 1982. Detection of a cytokeratin determinant common to diverse epithelial cells by a broadly cross-reacting monoclonal antibody. EMBO J. **1:**1429–1437.
14. **Goldman, R., and P. Steinert.** 1990. Cellular and molecular biology of intermediate filaments. Plenum Press, New York.
15. **Henderson, L., R. Benveniste, R. Sowder, R. Copeland, R. Schultz, and S. Oroszlan.** 1988. Molecular characterization of *gag* proteins from simian immunodeficiency virus ($SIV_{Mne}$). J. Virol. **62:**2587–2595.
16. **Jones, N., and T. Shenk.** 1979. Isolation of Ad5 host range deletion mutants defective transformation of rat embryo cells. Cell **17:**683–689.
17. **Moll, R., W. Franke, and D. Schiller.** 1982. The catalog of human cytokeratins: patterns of expression in normal epithelia, tumors and cultured cells. Cell **31:**11–24.
18. **Reich, N., P. Sarnow, E. Duprey, and A. J. Levine.** 1983. Monoclonal antibodies which recognize native and denatured forms of the adenovirus DNA-binding protein. Virology **128:**480–484.
19. **Shoeman, R., B. Höner, T. Stoller, C. Kesselmeier, M. Miedel, P. Traub, and M. Graves.** 1990. Human immunodeficiency virus type 1 protease cleaves the intermediate filament proteins vimentin, desmin, and glial fibrillary acidic protein. Proc. Natl. Acad. Sci. USA **87:**6336–6340.
20. **Shoeman, R., E. Mothes, B. Honer, C. Kesselmeier, and P. Traub.** 1991. Effect of human immunodeficiency virus type 1 protease on the intermediate filament subunit protein vimentin: cleavage, in vitro assembly and altered distribution of filaments in vivo following microinjection of protease. Acta Histochem. Suppl. **41:**129–141.
21. **Shoeman, R., E. Mothes, C. Kesselmeier, and P. Traub.** 1990. Intermediate filament assembly and stability in vitro: effect and implications of the removal of head and tail domains of vimentin by the human immunodeficiency virus type 1 protease. Cell Biol. Int. Rep. **14:**583–594.
22. **Staufenbiel, M., P. Epple, and W. Deppert.** 1986. Progressive reorganization of the host cell cytoskeleton during adenovirus infection J. Virol. **60:**1186–1191.
23. **Straus, S.** 1984. Adenovirus infections in humans, p. 153–178. *In* H. Ginsberg (ed.), The adenoviruses. Plenum Press, New York.
24. **Tölle, H., K. Weber, and M. Osborn.** 1987. Keratin filament disruption in interphase and mitotic cells—how is it induced? Eur. J. Cell Biol. **43:**35–47.
25. **Traub, P.** 1985. Intermediate filaments: a review. Springer-Verlag, Berlin.
26. **Vassar, R., P. Coulombe, L. Degenstein, K. Albers, and E. Fuchs.** 1991. Mutant keratin expression in transgenic mice causes marked abnormalities resembling a human genetic skin disease. Cell **64:**365–380.
27. **White, E., and R. Cipriani.** 1989. Specific disruption of intermediate filaments and the nuclear lamina by the 19-kD product of the adenovirus E1B oncogene. Proc. Natl. Acad. Sci. USA **86:**9886–9890.
28. **White, E., and R. Cipriani.** 1990. Role of adenovirus E1B proteins in transformation: altered organization of intermediate filaments in transformed cells that express the 19-kilodalton protein. Mol. Cell. Biol. **10:**120–130.
29. **Yeh-Kai, L., G. Akusjarvi, P. Alestron, U. Pettersson, M. Tremblay, and J. Weber.** 1983. Genetic identification of an endoproteinase encoded by the adenovirus genome. J. Mol. Biol. **167:**217–222.
30. **Zantema, A., J. Fransen, A. Davis-Olivier, F. Ramaekers, G. Vooijs, B. DeLeys, and A. van der Eb.** 1985. Localization of the E1B proteins of adenovirus 5 in transformed cells, as revealed by interaction with monoclonal antibodies. Virology **142:**44–58.
31. **Zhai, Z., X. Wang, and X. Qian.** 1988. Nuclear matrix-intermediate filament system and its alteration in adenovirus infected HeLa cell. Cell Biol. Int. Rep. **12:**99–108.